PHOTONICS Research

LED-pumped whispering-gallery laser

Simon J. Herr,[1] Karsten Buse,[1,2] and Ingo Breunig[1,2,*]

[1]Laboratory for Optical Systems, Department of Microsystems Engineering, University of Freiburg, Georges-Köhler-Allee 102, 79110 Freiburg, Germany
[2]Fraunhofer Institute for Physical Measurement Techniques IPM, Heidenhofstraße 8, 79110 Freiburg, Germany
*Corresponding author: ingo.breunig@imtek.uni-freiburg.de

Received 15 August 2017; revised 10 October 2017; accepted 11 October 2017; posted 12 October 2017 (Doc. ID 303819); published 2 November 2017

A low-cost light-emitting diode (LED) is sufficient to pump a quasi-continuous-wave bidirectional high-Q whispering-gallery resonator laser made of Nd:YVO_4. This is remarkable because of the very limited spatial and spectral coherence of an LED. The LED, delivering up to 3.5 W, centered around 810 nm, is turned on in intervals of 100 µs duration, and for these periods a laser output exceeding 0.8 mW has been verified. Furthermore, 0.1-s-long laser pulses are demonstrated. To the best of our knowledge, this is the first demonstration of an LED-pumped high-Q whispering-gallery laser. The concept can be extended easily to other laser active materials. A prospect is also to pump several of such lasers with a single LED.

OCIS codes: (140.3530) Lasers, neodymium; (140.3580) Lasers, solid-state; (140.3948) Microcavity devices; (230.3670) Light-emitting diodes.

https://doi.org/10.1364/PRJ.5.000B34

1. INTRODUCTION

Lasing in whispering-gallery resonators (WGRs) was observed shortly after the invention of the first laser [1]. Meanwhile, lasing in WGRs is reported in numerous materials, like liquids [2,3], glasses [4,5], wide bandgap crystals [6,7], polymers [8,9], and semiconductors [10,11]; see also Ref. [12] and references therein. Because of their high quality factor (Q-factor) and small mode volume, WGRs are ideal for low-threshold and narrow-linewidth lasers. Besides the generation of laser light, which is the key ingredient for many optical applications, WGR-based lasers are promising for high-precision sensing [12,13]. Furthermore, their applicability can be enlarged by intra-cavity frequency conversion [14]. In experiments where controlled coupling is a prerequisite, solid-state WGRs are best suited. Among those, highest Q-factors are achieved in glasses and wide bandgap crystals [15,16]. Typically, solid-state-based WGR lasers are pumped resonantly by exciting whispering-gallery modes (WGMs) close to the absorption wavelength of the laser-active material. This approach provides maximum excitation efficiency at the expense of the need of an external laser source, whose light frequency must be matched to the optical resonance frequency of the pump WGM. Thus, a narrow-linewidth and frequency tunable laser source is required. In the case of a large round-trip loss, the pump WGMs are spectrally broadened, which softens the requirement of temporal coherence of the external excitation laser [4,14]. However, one still has to fulfil the resonance condition of the cavity. To become independent of whispering-gallery pump modes, non-resonant direct illumination of the WGR is the most obvious strategy. Actually, flash-lamp pumping was applied in the very first demonstration of lasing in WGMs [1]. A different approach exploits the cascaded energy transfer between multiple layers of organic dyes, deposited on a WGR, allowing for non-resonant and broadband excitation [17]. Here, we demonstrate bidirectional lasing in a crystalline high-Q WGR, made of Nd:YVO_4, which is optically pumped by the spatially and temporally incoherent light of a single low-cost light-emitting diode (LED). Because of the high Q-factor of the cavity, a low-intensity source like an LED without any focusing optics is shown to be sufficient to achieve lasing. The continuing trend of LEDs to become more powerful will allow in the future for full-continuous-wave (cw) LED-pumped WGR lasers delivering several milliwatts of output power at low cost and with high reliability. Mirror-based LED-pumped bulk lasers have attracted much interest within recent years [18–23]. This report is organized as follows. First, we estimate the LED emission power that is required to reach the laser threshold. Then, we describe the experimental setup and present experimental data, which show good agreement with theoretical estimations. Finally, general conclusions are drawn.

2. ESTIMATION OF THE LASER THRESHOLD

In the following, we consider an Nd:YVO_4 WGR with an intrinsic Q-factor Q_{int} of 2×10^7. The major radius R and the minor radius r are 0.4 and 0.1 mm, respectively. The LED emission power, necessary to reach the laser threshold, can

be estimated from basic principles [24]: As the neodymium ion features a four-level system, we can assume the small signal gain γ_0 to be $\gamma_0 = \sigma_{em}\Delta N$, where σ_{em} is the laser-transition emission cross section and ΔN represents the population inversion density of the laser transition, having the dimension of cm^{-3}. Let δ be the combined loss coefficient of the WGR at the laser emission wavelength averaged over one round trip. It comprises absorption, scattering, radiation, and coupling losses. The loss coefficient δ can be expressed with the finesse F_l or the Q-factor of the loaded cavity Q_l as $\delta = 1/(F_l R)$ or $\delta = 2\pi n_l/(\lambda_l Q_l)$, with n_l being the refractive index of the host material at the lasing wavelength λ_l. Requesting equality of gain γ_0 and loss δ, one finds a critical inversion density of $\Delta N_{th} = 1/(F_l R\sigma_{em})$ or $\Delta N_{th} = 2\pi n_l/(\lambda_l Q_l \sigma_{em})$. Below the laser threshold, the population inversion density is related to the excitation pump rate J via the fluorescent lifetime of the laser transition τ: $\Delta N \approx J\tau$. The pump power P_p and the pump rate J are related to each other, $J = \lambda_p \eta P_p/(hcV_p)$. Here, $\lambda_p P_p/(hc)$ is the rate of pump photons passing through the volume of the WGM V_p, where h is the Planck constant, c is the vacuum speed of light, and λ_p is the vacuum wavelength of the pump light. The factor η accounts for a limited pump efficiency. It considers that only a fraction of the LED emission light is absorbed within the volume of the WGM. The volume of the WGMs V_p is given by their polar extent h_m, the radial extent w_m, and the circumference of the WGR: $V_p \approx 2\pi R h_m w_m$. The result for the threshold pump power P_{th} reads then as

$$P_{th} \approx \frac{2\pi h c h_m w_m}{\lambda_p \eta \sigma_{em} \tau F_l} \quad \text{or} \quad P_{th} \approx \frac{2\pi n_l h c V_p}{\lambda_l \lambda_p Q_l \eta \sigma_{em} \tau}. \tag{1}$$

The pump efficiency η considers two issues. 1) Which fraction of the pump light passes through the volume of the WGMs? 2) How much of this light is absorbed within the relevant volume? The polar and the radial extent h_m and w_m of WGMs for low polar and radial mode numbers with the given resonator dimensions are typically of the order of 20 and 10 μm, respectively [25]. For direct illumination of the WGR from the side, we estimate the spatial overlap of the pump light and the lasing modes to be the projection of the WGMs onto the LED chip with an active area A_{LED}. This estimation is feasible in the case that A_{LED} is in proximity to the WGR, as described in Section 3. Furthermore, we neglect refraction at the surface of the WGR, as an immersion fluid reduces refraction losses. Considering an LED chip with an edge length $\geq 2R$, a ratio of $2Rh_m/A_{LED}$ of the emitted pump light passes through the volume of the WGM. The Beer–Lambert law quantifies the absorption of the pump light within the relevant volume with $1 - \exp(-\alpha w_m)$, where α is the absorption coefficient of the WGR's material. The short absorption path and the absorption data presented in Fig. 1 justify the approximation $1 - \exp(-\alpha w_m) \approx \alpha w_m$, since $\alpha w_m \ll 1$ is valid. With this, the pump efficiency η reads as $\eta = 2Rh_m \alpha w_m/A_{LED}$.

As shown in Fig. 1, the light emitted by the LED has a spectral width of some tens of nanometers. Thus, we need to consider an effective absorption coefficient α_{eff}, which accounts for the broadband excitation light source as well as the wavelength and polarization-dependent absorption of Nd:YVO_4. In case of unpolarized light, α_{eff} can be written as

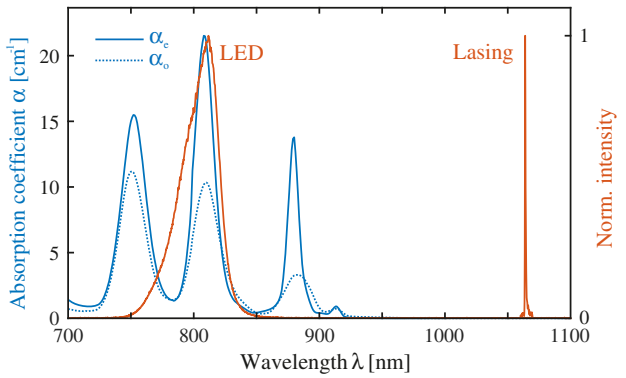

Fig. 1. Blue: measured absorption coefficient of Nd:YVO_4 for o- and e-polarized light α_o and α_e, respectively. Orange: normalized intensity profile of the LED at its maximum specified cw current of 0.8 A during cw operation, and normalized intensity profile of the WGR-laser emission in pulsed operation and an LED driving current >0.92 A.

$$\alpha_{eff} = \int_{0.7\ \mu m}^{0.9\ \mu m} \frac{\alpha_o(\lambda) + \alpha_e(\lambda)}{2} S_{LED}(\lambda) d\lambda \tag{2}$$

with

$$\int_{0.7\ \mu m}^{0.9\ \mu m} S_{LED}(\lambda) d\lambda = 1. \tag{3}$$

Here, $\alpha_o(\lambda)$ and $\alpha_e(\lambda)$ are the wavelength-dependent absorption coefficients of Nd:YVO_4 for ordinarily (o) and extraordinarily (e) polarized light, respectively, and $S_{LED}(\lambda)$ is the normalized spectral density, which represents the portion of the light power emitted by the LED in the wavelength interval from λ to $\lambda + d\lambda$. A representation of Eqs. (2) and (3) in the frequency space is equivalent. The absorption coefficients are measured by means of a grating spectrophotometer (Cary 500, Varian). Figure 1 shows $\alpha_o(\lambda)$ and $\alpha_e(\lambda)$ as well as the normalized intensity profile of the LED. With these values, one finds $\alpha_{eff} \approx 8.4\ cm^{-1}$ and $\eta \approx 1.3 \times 10^{-4}$ for an LED with $A_{LED} = 1\ mm^2$.

Considering $\eta = 2Rh_m \alpha_{eff} w_m/A_{LED}$, we can simplify Eq. (1) to

$$P_{th} \approx \frac{2\pi^2 n_l h c A_{LED}}{\lambda_l \lambda_p Q_l \sigma_{em} \tau \alpha_{eff}}, \tag{4}$$

which no longer contains any dependence on the spatial extent of the WGMs. This is plausible since we assumed a constant photon flux density of the pump light, and both the threshold pump power P_{th} and the absorbed power within the WGM are proportional to the mode volume V_p. The parameters in Eq. (4) are estimated as follows: The refractive index n_l of the host material at the lasing wavelength ($\lambda_l = 1064$ nm) for e-polarized light is 2.17 [26]. The emission cross section σ_{em} of the laser transition is $12 \times 10^{-19}\ cm^2$ [26]. We measure a fluorescent lifetime τ of 50 μs. In case of a critically coupled cavity, $Q_l = Q_{int}/2$ is valid. These numbers result in a P_{th} of approximately 0.2 W. Remarkably, this value is well achievable with LEDs.

3. SETUP DESCRIPTION

The spheroidally shaped WGR is fabricated from a 3% neodymium-doped z-cut yttrium vanadate crystal (Nd:YVO_4, Altechna). Shaping is done on a computer-controlled stage by means of femtosecond laser pulses (388 nm central wavelength, 2 kHz repetition rate, about 150 fs pulse duration, and about 300 mW of average power). Final polishing is done by hand. As the pump source we use a low-cost LED (SMB1N-810D, Roithner Lasertechnik). The peak emission wavelength is around 810 nm and the active area is specified with an output irradiance of 56 W/cm^2 at a constant current of 0.8 A, and a forward voltage of about 2 V. As the current source, we use a commercially available diode driver (ITC4020, Thorlabs). Silicone oil with a refractive index of about 1.4 between the LED and the WGR serves as an immersion medium to increase the coupling of the LED excitation light into the WGR. As the refractive index of the WGR host material is higher than the refractive index of the immersion fluid, the WGMs are still bound. The Q-factor is not affected. Evanescent coupling via a rutile prism extracts a fraction of the oscillating light. Also here, silicone oil increases the coupling strength. In the detection path, an aperture and a dielectric filter are used as spatial and frequency selective filters in order to detect the generated laser light. In this configuration (see Fig. 2), the WGR has an intrinsic Q-factor Q_{int} of about 2×10^7, at 980 nm wavelength. As we have no suitable light source at 1064 nm, we consider this a lower limit estimate for the Q-factor at the lasing wavelength, because 980 nm is closer to the absorption band being centered around 800 nm than the lasing wavelength is; see Fig. 1.

4. RESULTS

First, we operate the LED in quasi-cw mode, with current pulses as short as 100 μs at a repetition rate of 10 Hz. This avoids excessive heating and allows to study the turn-on behavior of the WGR laser. The peak current for driving the LED is varied between 0 and 5 A. Higher values damage the contact wires on the LED chip. Figure 3 presents the output power versus time for an LED driving current up to 1.5 A. At peak currents of up to 0.9 A, we observe low output powers of the order of a few microwatts, caused by fluorescence. Above 0.92 A, spiking occurs with rapidly increasing power.

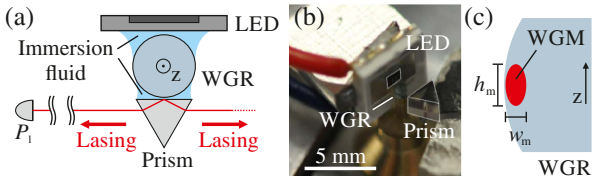

Fig. 2. (a) LED directly illuminates a laser-active WGR made out of z-cut Nd:YVO_4. Silicone oil serves as an immersion fluid to guide the light from the LED to the WGR. Evanescent coupling via a coupling prism extracts two counter-propagating laser beams stemming from the bidirectional lasing in WGMs. A detector (P_1) measures the laser output power. (b) Photograph of the experimental setup. The active area of the LED and the prism are highlighted. For the sake of recognizability, the prism is moved away from the resonator. (c) Illustration of the polar and the radial extents h_m and w_m of the WGMs, respectively.

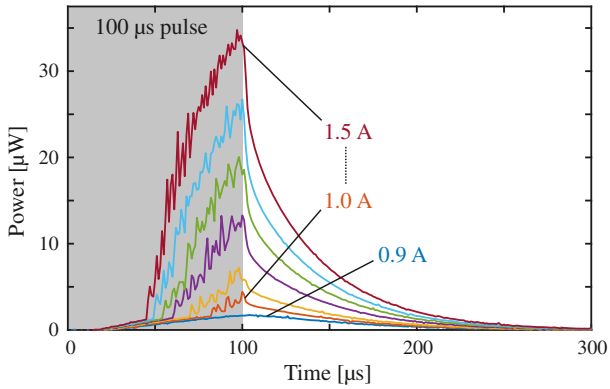

Fig. 3. Output power during a 100-μs-long excitation pulse. A low driving current of the LED yields fluorescent light. Above a threshold, laser spiking occurs, and the peak power is increasing rapidly with increasing current.

The threshold behavior and the laser spiking are clear indications for a laser process. Despite the high Q-factor, the cavity ringdown time is still much smaller than τ. Hence, the material is prone to laser spiking and relaxation oscillations. The LED driving current of 0.92 A corresponds to approximately 0.64 W pump power, which is remarkably close to the estimated pump threshold that we presented in Section 2. Within the gain bandwidth of Nd:YVO_4, which is about 257 GHz (≈1 nm) [27], the WGR possesses various WGMs. Hence, multimode laser operation and thermally induced mode hops can be expected. However, this is no fundamental limitation, as true cw pumping can allow us to reach a thermally steady state. Because of the limited spectral and temporal resolution of the spectrometer used for the data in Fig. 1, the number of lasing modes cannot be quantified.

In Fig. 4, we show the maximum output power versus LED driving current, for two different outcoupling strengths. The coupling strength can be varied by changing the gap between the WGR and the coupling prism. For stronger coupling, i.e., a small gap, the laser power exceeds 0.4 mW at the expense of

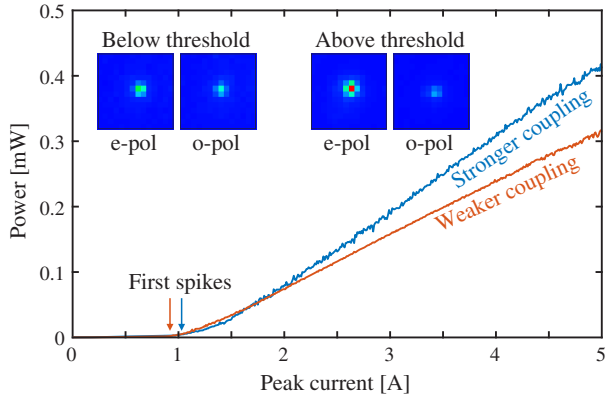

Fig. 4. Output peak power for 100-μs-long excitation pulses at different coupling strengths. Stronger coupling yields a higher laser output at an increased laser threshold compared to the case of weaker coupling. First laser spikes occur at 0.92 and 1.03 A. The insets illustrate the unpolarized emission below threshold and the e-polarized emission above the laser threshold. The pixel size is 2.2 μm × 2.2 μm.

an increased laser threshold. Here, first spikes are observed at an LED driving current of 1.03 A. It should be noted that the stated output power values correspond to only one single output path. As illustrated in Fig. 2, lasing occurs in the clockwise and counter-clockwise directions simultaneously, due to the rotational symmetry of the WGR. Hence, the total emitted laser power is twice as high as indicated in the figures. The insets in Fig. 4 show photographs of the coupling point of the WGR at the prism base. Below the laser threshold, similar amounts of e- and o-polarized light originate from the coupling point, indicating fluorescence activity. Above the laser threshold, e-polarized emission is clearly dominating. This is in accordance with the strongly polarization-dependent laser gain, which is maximum for e-polarized light. Considering the total lasing output power versus the LED driving current, we observe a slope of about 0.2 mW/A. With the LED specification (approximately 0.7 W/A), one can deduce an optical efficiency η_{optical} of about 2.9×10^{-4}. This is a lower limit estimate of η_{optical}, as the efficiency of the LED drops slightly for higher driving currents. With $\eta_{\text{optical}} = \eta\lambda_p/\lambda_l$, the experimentally determined value for η is about 3.8×10^{-4}. This value is consistent with the one estimated in Section 2, considering the undertaken simplifications.

LED-pumped lasing in the setup as it is presented here is not limited to 100-μs-long pulses. To verify this statement, we increase the excitation pulse length by three orders of magnitude to 0.1 s at a repetition rate of 1 Hz. As the LED is not cooled actively, we keep the driving current below 2 A. The temporal evolution of the detected power is presented in Fig. 5(a). Above a current of 0.9 A, laser spikes occur shortly after the LED is turned on. For a driving current close to the threshold, the laser oscillation stops during the presence of the excitation pulse, ending in fluorescent light emission. For currents of 1.2 A or more, laser oscillation is present during the whole excitation period.

The decaying power during the pulse can be attributed to three effects. 1) At elevated temperatures, the LED emission spectrum is redshifted, which lowers α_{eff} and, hence, also η. 2) Furthermore, the efficiency of the LEDs drops with increasing temperature. 3) The Q-factor decreases during the presence of the excitation pulse. From Fig. 5(b) it becomes obvious that the laser threshold is increasing over time. However, despite these detrimental effects, 100-ms-long laser pulses are achieved reliably. In the case that longer pulses or true-cw lasing is desired, an improved thermal management is supposed to resolve the present limitations.

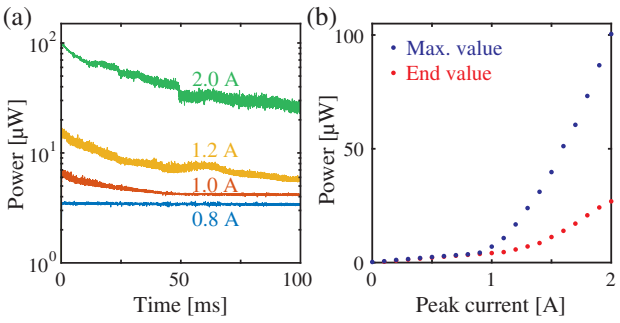

Fig. 5. (a) Output power during a 100-ms-long excitation pulse for different LED driving currents. Below 0.9 A, only fluorescent light is detected. Above 0.9 A, laser oscillation starts. (b) The blue data points indicate the maximum power of the pulse versus peak current. The red data points represent the end value, averaged over the last 10 ms of the pulse.

5. CONCLUSIONS

The concept of an LED-pumped WGR laser can be applied to other host materials, and is hence not limited to Nd:YVO_4. The suitability of a material as the host material for an LED-pumped WGR laser can be quantified by a figure of merit (FOM) that contains all relevant material properties and is derived directly from Eq. (4):

$$\text{FOM} = \frac{\lambda_l \lambda_p Q_l \sigma_{\text{em}} \tau \alpha_{\text{eff}}}{n_l}. \tag{5}$$

By comparing the FOM of the material of interest with the FOM of Nd:YVO_4, one can reliably predict the laser threshold of an LED-pumped WGR laser made out of the material of interest. A low FOM can be compensated for by obvious methods, like using multiple LEDs or brighter LEDs. A more advanced method for LED pumping of solid-state lasers employs luminescent concentrators [20]: recently, an output irradiance as high as 2.5 kW/cm^2 was achieved [23]. With these methods at hand, it can be expected that the concept of LED-pumped WGR lasers can be successfully applied to a variety of other laser-active materials. Application of a laser-active host material with a $\chi^{(2)}$ nonlinearity bears the potential for LED-pumped intra-cavity frequency conversion. A material of particular interest is neodymium-doped lithium niobate (Nd:MgO:$LiNbO_3$), whose FOM is only about one order of magnitude smaller than that of Nd:YVO_4 [14,28]. With this, LED-pumped frequency synthesizers come into reach, accessing the full wealth of nonlinear effects like their passive counterparts do [29] at, however, considerably reduced cost and complexity.

Funding. Deutsche Forschungsgemeinschaft (DFG) (BR 4194/6-1).

Acknowledgment. The authors thank C. S. Werner for fruitful discussions.

REFERENCES

1. C. G. B. Garrett, W. Kaiser, and W. L. Bond, "Stimulated emission into optical whispering modes of spheres," Phys. Rev. **124**, 1807–1809 (1961).
2. H.-M. Tzeng, K. F. Wall, M. B. Long, and R. K. Chang, "Laser emission from individual droplets at wavelengths corresponding to morphology-dependent resonances," Opt. Lett. **9**, 499–501 (1984).
3. S. X. Qian, J. B. Snow, H. M. Tzeng, and R. K. Chang, "Lasing droplets: highlighting the liquid-air interface by laser-emission," Science **231**, 486–488 (1986).
4. V. Sandoghdar, F. Treussart, J. Hare, V. Lef-vre-Seguin, J.-M. Raimond, and S. Haroche, "Very low threshold whispering-gallery-mode microsphere laser," Phys. Rev. A **54**, R1777 (1996).
5. L. Yang and K. J. Vahala, "Gain functionalization of silica microresonators," Opt. Lett. **28**, 592–594 (2003).
6. T. Baer, "Continuous-wave laser oscillation in a Nd:YAG sphere," Opt. Lett. **12**, 392–394 (1987).

7. T. Le, S. J. Schowalter, W. Rellergert, J. Jeet, G. Lin, N. Yu, and E. R. Hudson, "Low-threshold ultraviolet solid-state laser based on a Ce^{3+}:$LiCaAlF_6$ crystal resonator," Opt. Lett. **37**, 4961–4963 (2012).
8. M. Kuwata-Gonokami, S. Ozawa, R. H. Jordan, A. Dodabalapur, H. E. Katz, M. L. Schilling, and R. E. Slusher, "Polymer microdisk and microring lasers," Opt. Lett. **20**, 2093–2105 (1995).
9. M. Kuwata-Gonokami and K. Takeda, "Polymer whispering gallery mode lasers," Opt. Mater. **9**, 12–17 (1998).
10. S. L. McCall, A. F. J. Levi, R. E. Slusher, S. J. Pearton, and R. A. Logan, "Whispering-gallery mode microdisk lasers," Appl. Phys. Lett. **60**, 289–291 (1992).
11. H. Cao, J. Y. Xu, W. H. Xiang, Y. Ma, S.-H. Chang, S. T. Ho, and G. S. Solomon, "Optically pumped InAs quantum dot microdisk lasers," Appl. Phys. Lett. **76**, 3519–3521 (2000).
12. L. He, Ş. K. Özdemir, and L. Yang, "Whispering gallery microcavity lasers," Laser Photon. Rev. **7**, 60–82 (2013).
13. T. Reynolds, N. Riesen, A. Meldrum, X. Fan, J. M. M. Hall, T. M. Monro, and A. François, "Fluorescent and lasing whispering gallery mode microresonators for sensing applications," Laser Photon. Rev. **11**, 1600265 (2013).
14. S. J. Herr, Y. Folwill, K. Buse, and I. Breunig, "Self-frequency doubling in a laser-active whispering-gallery resonator," Opt. Lett. **42**, 2627–2630 (2017).
15. M. L. Gorodetsky, A. A. Savchenkov, and V. S. Ilchenko, "Ultimate Q of optical microsphere resonators," Opt. Lett. **21**, 453–455 (1996).
16. A. A. Savchenkov, V. S. Ilchenko, A. B. Matsko, and L. Maleki, "Kilohertz optical resonances in dielectric crystal cavities," Phys. Rev. A **70**, 051804 (2004).
17. C. Rotschild, M. Tomes, H. Mendoza, T. L. Andrew, T. M. Swager, T. Carmon, and M. A. Baldo, "Cascaded energy transfer for efficient broad-band pumping of high-quality, micro-lasers," Adv. Mater. **23**, 3057–3060 (2011).
18. A. Barbet, F. Balembois, A. Paul, J.-P. Blanchot, A.-L. Viotti, J. Sabater, F. Druon, and P. Georges, "Revisiting of LED pumped bulk laser: first demonstration of Nd:YVO_4 LED pumped laser," Opt. Lett. **39**, 6731–6734 (2014).
19. B. Villars, E. S. Hill, and C. G. Durfee, "Design and development of a high-power LED-pumped Ce:Nd:YAG laser," Opt. Lett. **40**, 3049–3052 (2015).
20. A. Barbet, A. Paul, T. Gallinelli, F. Balembois, J.-P. Blanchot, S. Forget, S. Chénais, F. Druon, and P. Georges, "Light-emitting diode pumped luminescent concentrators: a new opportunity for low-cost solid-state lasers," Optica **3**, 465–468 (2016).
21. K.-Y. Huang, C.-K. Su, M.-W. Lin, Y.-C. Chiu, and Y.-C. Huang, "Efficient 750-nm LED-pumped Nd:YAG laser," Opt. Express **24**, 12043–12054 (2016).
22. C. Y. Cho, C. C. Pu, K. W. Su, and Y. F. Chen, "LED-side-pumped Nd:YAG laser with >20% optical efficiency and the demonstration of an efficient passively Q-switched LED-pumped solid-state laser," Opt. Lett. **42**, 2394–2397 (2017).
23. P. Pichon, A. Barbet, D. Blengino, P. Legavre, T. Gallinelli, F. Druon, J.-P. Blanchot, F. Balembois, S. Forget, S. Chénais, and P. Georges, "High-radiance light sources with LED-pumped luminescent concentrators applied to pump Nd:YAG passively Q-switched laser," Opt. Laser Technol. **96**, 7–12 (2017).
24. B. E. A. Saleh and M. C. Teich, *Fundamentals of Photonics* (Wiley, 2007).
25. I. Breunig, B. Sturman, F. Sedlmeir, H. G. L. Schwefel, and K. Buse, "Whispering gallery modes at the rim of an axisymmetric optical resonator: analytical versus numerical description and comparison with experiment," Opt. Express **21**, 30683–30692 (2013).
26. H. R. Xia, X. L. Meng, M. Guo, L. Zhu, H. J. Zhang, and J. Y. Wang, "Spectral parameters of Nd-doped yttrium orthovanadate crystals," J. Appl. Phys. **88**, 5134–5137 (2000).
27. T. Taira, A. Mukai, Y. Nozawa, and T. Kobayashi, "Single-mode oscillation of laser-diode-pumped Nd:YVO_4 microchip lasers," Opt. Lett. **16**, 1955–1957 (1991).
28. T. Y. Fan, A. Cordova-Plaza, M. J. F. Digonnet, R. L. Byer, and H. J. Shaw, "Nd:MgO:$LiNbO_3$ spectroscopy and laser devices," J. Opt. Soc. Am. B **3**, 140–148 (1986).
29. I. Breunig, "Three-wave mixing in whispering gallery resonators," Laser Photon. Rev. **10**, 569–587 (2016).